



Evaluating vegetation–hydrology interactions in Mediterranean catchments using the distributed ecohydrological model MEDFATELAND

María González-Sanchis^{1,2,3}, Miquel De Cáceres^{1,4}, Paula Martín¹, Gemma Piqué¹, Pau Garcia Iñurria¹, and Susan Manrique^{1,5}

¹Ciència i Tecnologia Forestal de Catalunya (CTFC), Solsona, Spain

²Department of Vegetal Production, Universitat Politècnica de València, València, Spain

³Forest Bioengineering Solutions, Solsona, Spain

⁴CREAF-CSIC, Cerdanyola del Vallès, Barcelona, Spain

⁵Forest Research Centre, School of Agriculture, University of Lisbon, Lisbon, Portugal

Correspondence: María González-Sanchis (mariadelcarmen.gonzalez@ctfc.cat)

Abstract. Mediterranean forest ecosystems strongly regulate catchment hydrology through vegetation-driven processes such as rainfall interception, transpiration, and soil water uptake. In recent decades, increasing forest density following land abandonment has altered water balances across many Mediterranean basins, raising concerns about declining streamflow and increasing drought vulnerability. Process-based ecohydrological models provide a valuable framework for investigating these coupled vegetation–water dynamics and exploring potential management strategies. A spatially distributed implementation is particularly valuable because it allows representing within-catchment heterogeneity, evaluating predicted vegetation dynamics against remotely sensed products, and—crucially—enabling spatially explicit forest management scenarios in which species-specific treatments are applied heterogeneously across space.

In this study, the distributed ecohydrological model MEDFATELAND is presented and applied at watershed scale in Mediterranean catchments (Aigua d’Ora and Siurana) in northeastern Spain. The objectives were (i) to evaluate the ability of the model to reproduce observed hydrological and vegetation dynamics, (ii) to analyze the relationships between vegetation structure and catchment water balance under current conditions, and (iii) to assess the potential effects of forest management on water availability, plant water stress, fuel moisture, and fire behavior.

Model calibration using daily streamflow resulted in moderate performance at the daily scale (NSE = 0.49 in Aigua d’Ora and 0.15 in Siurana) and improved skill at the monthly scale (NSE = 0.62 and 0.46, respectively). Independent evaluation against remotely sensed data showed that simulated gross primary production (GPP) reproduced observed temporal variability reasonably well, while simulated leaf area index (LAI) showed greater spatial variability. Historical trend analyses over the 2001–2023 observation period indicated increasing LAI without significant trends in precipitation or temperature, accompanied by a decline in river discharge, suggesting that vegetation structural changes may be contributing to increased catchment water consumption.

Scenario simulations indicated that forest management reduced canopy structure and interception while increasing blue water fluxes (runoff and deep drainage) in both catchments. The hydrological response was stronger in the wetter Aigua d’Ora



basin and more modest in the drier Siurana basin, highlighting the interplay between climate, vegetation composition, and the spatial extent of treatments on catchment-scale outcomes.

25 Overall, the results demonstrate that MEDFATELAND can realistically represent coupled vegetation–hydrology dynamics at watershed scale and provides a useful tool for evaluating forest management strategies aimed at improving water availability and reducing wildfire risk in Mediterranean environments.

1 Introduction

30 Mediterranean ecosystems are characterized by strong climatic seasonality, recurrent droughts, and pronounced interannual variability in water availability, making water a primary limiting factor for both ecosystem functioning and human activities. In these environments, vegetation plays a central role in regulating catchment hydrology through rainfall interception, transpiration, and soil water uptake processes. Consequently, understanding forest–water interactions is essential for predicting hydrological responses to environmental change and for designing sustainable land management strategies (Bosch and Hewlett, 35 1982; Brown et al., 2005).

Over recent decades, widespread forest expansion and increasing canopy density across Mediterranean regions have altered catchment water balances (García-Ruiz et al., 2011; Lasanta et al., 2017). Numerous studies have shown that increases in forest biomass tend to reduce water yield through enhanced evapotranspiration, while vegetation removal or thinning can redistribute water toward runoff and groundwater recharge (Farley et al., 2005; Ukkola et al., 2016). At the same time, forest structure 40 strongly influences wildfire behavior by modifying fuel continuity, canopy moisture, and energy exchange within stands (Agee and Skinner, 2005). These interactions highlight the need for integrated approaches capable of simultaneously analysing the interplay between hydrological, ecological, and fire-related processes.

Ecohydrological models provide a powerful framework for representing the feedbacks between vegetation dynamics and hydrological processes across spatial and temporal scales (Sun et al., 2023). Process-based models allow testing hypotheses that 45 cannot be directly evaluated through observations alone, particularly regarding long-term ecosystem responses and alternative management scenarios. However, applying process-based ecohydrological models that explicitly represent vegetation dynamics at the watershed scale remains challenging, especially in Mediterranean environments where strong climate variability and heterogeneous landscapes complicate model transferability and evaluation (Ruiz-Pérez et al., 2017; Fatichi et al., 2016a). A key question in this context concerns the appropriate spatial structure of the hydrological (sub-)model design. While lumped 50 (catchment-averaged) models can reproduce outlet discharge reasonably well, they cannot explicitly represent strong within-catchment heterogeneity—such as gradients in elevation, aspect, soils, and species composition—that generate large spatial contrasts in water balance and vegetation functioning (Beven, 2012; Clark et al., 2015; García-Ruiz et al., 2011; Fatichi et al., 2016b). Semi-distributed approaches partially address this limitation by aggregating heterogeneity into hydrological response



units, but they still lack the spatial resolution needed for grid-cell evaluation against satellite products or spatially heterogeneous
55 management interventions. Fully distributed models, by contrast, enable quantification of how local changes in vegetation
structure at the stand scale propagate to catchment-scale partitioning between evapotranspiration, runoff, and deep drainage,
and how they shape spatial patterns of vegetation water status and fire-relevant indicators (Fatichi et al., 2016a; Pappas et al.,
2015).

MEDFATE is a process-based model designed to simulate forest functioning and dynamics with a special focus on Mediter-
60 ranean areas (De Cáceres et al., 2015, 2021, 2023). The model performs energy, water, and carbon balances in forest stands
given soil, vegetation, and daily weather inputs. Vegetation is represented using a cohort-based approach in which groups of
individuals of the same size and species identity compete for light and water resources. MEDFATE has been applied to esti-
mate how forest structure and forest management affect water partitioning, plant drought stress, and potential wildfire behavior
at the stand scale (De Cáceres et al., 2021, 2023). Here we present MEDFATELAND, a watershed-scale model that extends
65 the MEDFATE framework by coupling stand-level processes with spatially distributed hydrological processes within a grid-
ded catchment representation, enabling the analysis of coupled vegetation–water interactions and management impacts at the
catchment scale.

This integration enables MEDFATELAND to simulate how changes in vegetation structure propagate to catchment-scale
water partitioning (evapotranspiration, runoff, and deep drainage) while simultaneously producing fire-relevant indicators de-
70 rived from canopy and surface fuel conditions. In contrast to catchment-aggregated models calibrated only at the outlet, the
distributed configuration allows evaluation of emergent vegetation dynamics against independent remotely sensed products
(LAI and GPP) and supports spatially heterogeneous, species-specific management interventions triggered by local structural
thresholds. The present study therefore provides the first watershed-scale evaluation of the MEDFATE modelling framework
in Mediterranean catchments, demonstrating its suitability for integrated assessment of vegetation–water interactions and man-
75 agement trade-offs under drought and wildfire risk. The objectives are threefold: (i) to evaluate the ability of the model to re-
produce observed hydrological and vegetation dynamics using independent datasets; (ii) to use the validated model to analyse
forest–water relationships under current conditions; and (iii) to explore how alternative forest management strategies influence
water balance, ecosystem productivity, and fire-related variables.

2 Study Sites

80 The study was conducted in two Mediterranean mountain catchments located in Catalonia (northeastern Iberian Peninsula):
the Aigua d’Ora and Siurana basins. The selected study areas correspond to upstream sub-catchments defined by hydrological
control points, allowing comparison of eco-hydrological processes under contrasting climatic and management conditions (see
Table 1 for main physiographic and climatic characteristics of both study sites).

[Figure 1 about here.]



85 2.1 Aigua d’Ora Catchment

The Aigua d’Ora catchment is situated in the Pre-Pyrenean region of central Catalonia and forms part of the Llobregat River drainage system via the Cardener River. Analyses were restricted to the upper Aigua d’Ora basin (12 575 ha), extending from the headwaters to the Navés gauging station (station code: EA063), which defines the downstream boundary of the study area.

90 The basin drains steep mountainous terrain characterized by narrow valleys and relatively high elevations. Land cover is predominantly forested. Vegetation is mainly composed of *Pinus sylvestris* and *Pinus nigra*, which represent the most abundant tree species, while *Pinus uncinata* occurs locally at higher elevations and cooler sites. Current forest cover largely reflects natural succession following historical agricultural abandonment typical of Mediterranean mountain regions.

100 The climate is Mediterranean with continental and montane influence. Mean annual precipitation is approximately 766 mm, with rainfall concentrated in spring and autumn and marked summer droughts. Mean daily minimum temperature is $4.9 \pm 5.6^\circ\text{C}$, while mean daily maximum temperature reaches $14.5 \pm 7.2^\circ\text{C}$. Streamflow exhibits strong seasonal variability, with low flows during summer and rapid hydrological responses to episodic rainfall events. Hydrological regulation within the studied section is minimal, and discharge dynamics largely reflect natural climatic forcing.

2.2 Siurana Catchment

100 The Siurana catchment is located in Tarragona province in southwestern Catalonia and belongs to the Ebro River basin. The study area corresponds to the upstream portion of the basin draining to the Siurana reservoir (6 075 ha), which constitutes the hydrological outlet of the analysed catchment.

105 The basin is characterized by rugged topography associated with the Prades and Montsant mountain ranges, transitioning downstream into agricultural landscapes dominated by vineyards and olive groves typical of the Priorat region, together with Mediterranean shrublands and forest patches. Forest vegetation is mainly composed of drought-adapted Mediterranean species, particularly *Pinus halepensis* and *Quercus ilex*, which dominate many forested areas and reflect the relatively dry climatic conditions of the basin.

110 The climate is Mediterranean and comparatively dry, with strong interannual rainfall variability and recurrent summer droughts. Mean annual precipitation is approximately 530 mm. Mean daily minimum and maximum temperatures are $7.2 \pm 5.7^\circ\text{C}$ and $18.3 \pm 7.3^\circ\text{C}$, respectively. Streamflow regimes are influenced by reservoir regulation, which modifies natural discharge variability and supports downstream water management.

2.3 Comparative Context

115 The two study catchments represent contrasting Mediterranean hydro-climatic settings spanning a precipitation gradient from relatively humid pre-Pyrenean conditions (Aigua d’Ora, 766 mm yr^{-1}) to drier inland Mediterranean environments (Siurana, 530 mm yr^{-1}). Differences in temperature regimes further highlight this climatic gradient, providing a suitable framework for investigating hydrological and ecological responses to varying water availability and management regimes. These contrasting climatic conditions, together with the associated differences in vegetation structure described above, make the two basins



an appropriate natural laboratory for analysing ecohydrological processes across Mediterranean environments with differing degrees of water limitation.

[Table 1 about here.]

120 3 Material and Methods

3.1 Eco-hydrological analysis

To characterize the current hydrological status of both catchments and their evolution over the past two decades, temporal trends in water discharge, drought conditions, air temperature, and vegetation dynamics were analyzed. Streamflow was evaluated at a daily time step using observations provided by the River Basin Authority “Agència Catalana de l’Aigua” at the outlets of the simulation domains. In Aigua d’Ora, observations correspond to river discharge measured at the Navés gauging station. In Siurana, the outlet is the Siurana reservoir and the available hydrological record corresponds to daily variations in reservoir storage (volume change), which integrates catchment inflows and regulated outflows. Therefore, the hydrological evaluation in Siurana is interpreted as the model’s capacity to reproduce catchment-scale water balance dynamics under reservoir control, rather than natural (unregulated) streamflow variability.

130 Long-term temporal trends were assessed using the non-parametric Mann–Kendall test (Mann, 1945; Kendall, 1975), which is suitable for auto-correlated and non-normally distributed hydro-meteorological time series. The test evaluates the null hypothesis of no monotonic trend against the alternative of a significant increasing or decreasing trend. Trends were considered statistically significant at $\alpha = 0.05$, and the magnitude of significant trends was estimated using Sen’s non-parametric slope estimator (Sen, 1968), which calculates the median slope of all pairwise data combinations and is robust to outliers and missing values.

140 For spatially distributed variables (meteorological variables: daily minimum and maximum air temperature, precipitation; and vegetation dynamics: LAI and GPP), Kendall’s τ statistic and the associated two-sided p -value were computed independently at each grid cell. Spatial distributions of Kendall’s τ and Sen’s slope were then mapped by joining trend statistics to the corresponding grid-cell centroids, allowing identification of spatially coherent patterns of change. River discharge, available as a single catchment-outlet time series, was analysed at the catchment level only.

All analyses were performed at the daily time step. To isolate inter-annual variability from the seasonal cycle, anomaly series were additionally computed by subtracting the long-term mean day-of-year climatology from each daily value prior to trend estimation. All analyses were implemented in R (R Core Team, 2024) using the `Kendall` (McLeod, 2011) and `trend` (Pohlert, 2023) packages.

145 Drought dynamics were assessed by computing the Standardized Precipitation Index (SPI) from daily precipitation records obtained from METEOCAT weather stations. Temperature and precipitation trends were derived from METEOCAT observations. Vegetation trends were analyzed using MODIS-derived LAI (MOD15A2H) and GPP (MOD17A2H) products for the period 2001–2023 at an 8-day temporal resolution.



3.2 MEDFATE and MEDFATELAND

150 MEDFATE is a process-based model designed to simulate forest functioning and dynamics with a special focus on Mediter-
ranean areas. The model performs energy, water, and carbon balances in forest stands given appropriate soil, vegetation, and
daily weather inputs. Vegetation is represented using a set of woody plant cohorts representing individuals of the same size
and species identity. Soils are stratified into a set of user-defined layers with different textural and structural properties, often
including a rocky layer down to several meters depth. Plant cohorts can have different vertical distributions of roots among
155 soil layers; in the version used here (medfate v. 4.8.4), root systems of different cohorts fully overlap horizontally by default,
meaning they compete for water from shared soil pools. MEDFATE can perform water balance using different levels of mech-
anistic detail depending on sub-model choices for energy balance, plant transpiration (including explicit plant hydraulics), and
bulk soil water fluxes.

MEDFATELAND is a novel component of the MEDFATE modelling framework designed to extend the capabilities of
160 MEDFATE to a spatially explicit context. Among other capabilities, MEDFATELAND allows coupling local water balance
processes in a gridded landscape representation with spatially distributed hydrological processes, enabling the analysis of
coupled vegetation–water interactions and management impacts at the catchment scale. In MEDFATELAND, grid cells are
classified as either wildland (for forests, shrublands, or grasslands), agriculture, rock, artificial, or water. Vertically, the model
represents a snowpack compartment, different soil layers, and a groundwater (i.e., aquifer) compartment beyond the reach of
165 plant roots. Wildland and agriculture cells represent soil layers vertically coupled to a deep aquifer compartment. While local
water balances in wildland cells directly follow the MEDFATE design, the local water balance of agriculture cells follows the
same design for soil hydraulic processes but with transpiration estimated using potential evapotranspiration and crop factors.
Rock, artificial, and water cells do not include soil processes but can include snowpack dynamics and allow direct drainage
towards the aquifer compartment.

170 The design of lateral flows in MEDFATELAND distinguishes between: (a) overland surface flows from upper to lower
elevation cells; (b) lateral saturated soil flows (interflow) between adjacent cells; and (c) lateral groundwater flow (baseflow)
between adjacent cells. Routing of overland surface flows follows T-HYDRO (Ostendorf and Reynolds, 1993). Subsurface
flows (i.e. interflow and baseflow) are modelled following the kinematic wave approximation of DHSVM (Wigmosta et al.,
2002). Channel routing is performed afterwards by calculating an average flow velocity of the whole channel network according
175 to Manning’s equation when a river network is specified. Groundwater losses towards a deeper, disconnected aquifer can
also be simulated. A split-parameter parametrization inspired by the approach of Francés et al. (2007) reduces the number
of parameters to be calibrated, focusing on multipliers for saturated soil conductivity (vertical and lateral flows) and lateral
groundwater conductivity. Full technical details of MEDFATE and MEDFATELAND are available at [https://emf-creaf.github.
io/medfatebook/](https://emf-creaf.github.io/medfatebook/).

180 In this study, water balance was performed using the Richards 1D sub-model for soil hydraulics and the Granier sub-model
for plant transpiration. Landscape-scale simulations were run using the `fordyn_land()` function of the `medfateland`
package. The R package versions used were `medfate v. 4.8.4` and `medfateland v. 2.8.1`.



3.2.1 Model inputs

MEDFATELAND requires daily climatic data, soil characteristics, vegetation biophysical parameters, and a Digital Ter-
185 rain Model (DTM). Climatic data were obtained from METEOCAT weather stations and spatially interpolated using the
`meteoland` R package (De Caceres et al., 2018). Soil parameters (texture, bulk density, and rock fragment content) were
derived from SoilGrids. The DTM was derived from airborne LiDAR data collected in 2015 by PNOA, with a point density of
2 points m^{-2} and vertical errors below 40 cm. The model was applied at a spatial grid resolution of 500 m.

The vegetation characterization was developed using data from the Spanish National Forest Inventory (IFN3), corresponding
190 to the survey carried out around the year 2000. These data provide information on forest composition and structure (species
presence, tree density, DBH, height, and basal area) used to derive the vegetation biophysical parameters required by the model.
IFN3 plot data were spatially assigned to model grid cells using Thiessen (Voronoi) polygons, whereby each cell was attributed
the vegetation parameters of its nearest IFN3 plot. The resulting vegetation map was subsequently corrected using the Spanish
Forest Map (Mapa Forestal de España), which was used to identify and reclassify non-forested grid cells: cells corresponding
195 to agricultural land were assigned as agriculture cells and those dominated by bare rock or rocky outcrops were assigned as
rock cells. No urban or artificial surfaces were identified within the study catchments, so no artificial cell type was required.
The final land-cover map therefore includes wildland (forest and shrubland), agriculture, and rock cell types, reflecting the
heterogeneous landscape composition of both catchments.

3.2.2 Calibration and evaluation of MEDFATELAND

200 Manual calibration was conducted using daily simulated and observed streamflow data. The calibration period covered 2000–
2012, while the independent evaluation period spanned 2013–2023. The calibration focused on a reduced set of physically
meaningful parameters controlling vertical and lateral water fluxes within the soil and groundwater compartments, following a
split-parameter approach similar to that of Francés et al. (2007).

Specifically, the following parameters were manually adjusted: (i) the exponent regulating the dependence of lateral interflow
205 transmissivity on soil saturation, $n_{\text{interflow}}$; (ii) the exponent controlling the dependence of groundwater transmissivity on
aquifer storage, n_{baseflow} ; and (iii) a set of multiplicative correction factors applied to hydraulic conductivities, including
vertical soil conductivity ($R_{\text{localflow}}$), lateral soil conductivity ($R_{\text{interflow}}$), and lateral groundwater conductivity (R_{baseflow}). In
addition, the deep aquifer loss coefficient (D_{loss}) and the Manning roughness coefficient for the river channel (n_{Manning}) were
calibrated.

210 Model performance during calibration and evaluation was assessed by comparing daily simulated and observed stream-
flow using multiple goodness-of-fit metrics, including the Nash–Sutcliffe Efficiency (NSE), Kling–Gupta Efficiency (KGE),
coefficient of determination (R^2), Pearson correlation coefficient (r), and root mean square error (RMSE).

To further evaluate model performance in terms of vegetation dynamics, a spatially explicit validation was performed through
pixel-wise comparisons of simulated and observed monthly leaf area index (LAI) and gross primary productivity (GPP). Ob-



215 servational datasets were obtained from MODIS products (MOD15A2H and MOD17A2H) for the period 2001–2023. Finally,
temporal trends in river discharge, LAI, and GPP were analysed and contrasted against observed time series.

3.2.3 Model application and forest management scenario

After the calibration and evaluation phases, MEDFATELAND was applied over the same 2000–2023 simulation period to
assess the potential effects of forest management on the eco-hydrological dynamics of both catchments. For each catchment,
220 a single forest management scenario was implemented and compared with the current vegetation conditions (baseline). The
objective was to explore whether the proposed management actions could improve eco-hydrological functioning, while evalu-
ating the capacity of the distributed MEDFATELAND model to capture the catchment-scale consequences of realistic thinning
prescriptions.

The scenario focused on the dominant forest species: *Pinus halepensis*, *Pinus nigra*, *Pinus sylvestris*, *Pinus uncinata*, and
225 *Quercus ilex*. Management prescriptions were based on eco-hydrological silvicultural guidelines and implemented through
species-specific thinning operations triggered when stand basal area exceeded a species-specific threshold; once triggered,
a fixed percentage of basal area was removed with a minimum five-year interval between interventions. The aim was not
to identify an optimal strategy but to evaluate whether MEDFATELAND can capture the ecohydrological consequences of
realistic landscape-scale treatments. The main prescriptions are summarized in Table 2.

230 Model outputs were analyzed focusing on key variables related to water balance and fire hazard, including runoff, deep
percolation, soil water content, fuel moisture, and fire behavior indicators. To strengthen the process-based interpretation,
results were analyzed following a mechanistic pathway linking canopy structure to (i) water partitioning and (ii) fire behavior. In
addition to whole-period averages, results were contrasted with a summer-period subset (June–August) to emphasize conditions
when evaporative demand peaks and wildfire risk is highest. Fire behavior indicators were interpreted using Byram intensity
235 (Byram, 1959), with $I_{b,crown}$ and $I_{b,surface}$ representing crown and surface fire line intensity, and CFP and SFP representing
crown and surface potential fire, respectively.

[Table 2 about here.]

4 Results

4.1 Trend and drought analysis

240 Trend analyses indicate that daily precipitation did not exhibit a statistically significant long-term trend in either catchment
over the study period. Nevertheless, analysis of the Standardized Precipitation Index at the 12-month scale (SPI-12) revealed
pronounced multi-annual hydroclimatic variability in both basins (Fig. 2). Several drought episodes were identified, with
two major events affecting both catchments around 2005–2007 and 2022–2024, when SPI values dropped below the drought
threshold ($SPI < -1$). The mid-2000s drought was particularly intense, with SPI values locally falling below -2 , indicating
245 severe drought conditions, especially in the Siurana catchment. The most recent drought appears more persistent, with negative



SPI values extending over multiple consecutive months from 2022 onwards. Between these dry phases, wetter periods were also observed, notably around 2003–2004, 2009–2010, and 2018–2020, when SPI values exceeded +2. Overall, the SPI time series highlights strong interannual variability characterized by alternating wet and dry periods rather than a monotonic climatic trend.

250

[Figure 2 about here.]

Vegetation dynamics showed contrasting behavior between structural and physiological indicators. LAI displayed a statistically significant increasing trend across large portions of both catchments, indicating progressive canopy densification during the last two decades. In contrast, GPP exhibited a weak positive trend that was not statistically significant, suggesting that structural vegetation changes were not accompanied by proportional increases in ecosystem carbon assimilation (see Figure

255

3).

[Figure 3 about here.]

Temperature variables (daily mean, maximum, and minimum air temperature) did not show significant trends over the analysis period ($p > 0.05$). Despite this relative hydro-climatic stability, daily river discharge exhibited a significant decreasing trend in both catchments, indicating potential changes in ecohydrological regulation at the basin scale.

260 4.2 Model performance

The final set of calibrated parameters for each catchment is reported in Table 3. These values reflect the dominant hydrological processes controlling water flux partitioning in each system.

[Table 3 about here.]

Notably, the Siurana catchment exhibits a markedly lower $n_{\text{interflow}}$ value, indicating a reduced sensitivity of lateral soil water fluxes to saturation conditions compared to Aigua d’Ora. Additionally, the lower deep aquifer loss coefficient in Siurana suggests a more limited percolation towards deep groundwater compartments, consistent with its more constrained and regulated hydrological response.

265

These parameter differences help explain the contrasting model performance between catchments. In Aigua d’Ora, the higher sensitivity of interflow to soil moisture promotes a more dynamic lateral redistribution of water, improving the simulation of peak flows and temporal variability. In contrast, the reduced interflow sensitivity and lower deep losses in Siurana reflect a system dominated by storage buffering and regulation effects, which dampens short-term variability and contributes to lower model skill at the daily scale.

270

From a sensitivity perspective, model performance was found to be particularly responsive to parameters controlling lateral fluxes ($n_{\text{interflow}}$, $R_{\text{interflow}}$) and groundwater dynamics (n_{baseflow} , R_{baseflow}), as these directly influence flow generation and recession behavior. In contrast, parameters such as n_{Manning} and $R_{\text{localflow}}$ exerted a comparatively lower influence on aggregated performance metrics, mainly affecting routing and vertical redistribution processes.

275



4.2.1 Hydrological calibration and validation using outlet hydrological observations

Model performance was evaluated at both daily and monthly temporal resolutions using NSE, KGE, R^2 , Pearson r , and RMSE; these values are reported in Table 4.

280 [Table 4 about here.]

In the Aigua d’Ora catchment, the model achieved moderate performance at the daily scale, with an NSE of 0.49 and a KGE of 0.61. The corresponding R^2 and Pearson correlation were 0.57 and 0.75, respectively, indicating that the model reproduced the temporal variability of daily discharge reasonably well. At the monthly scale, model performance improved substantially, with NSE = 0.62 and KGE = 0.56, $R^2 = 0.75$, Pearson $r = 0.87$, and RMSE decreasing from 0.59 to 0.39 (see Fig. 4).

285 [Figure 4 about here.]

In the Siurana catchment, daily simulations showed lower skill (NSE = 0.15; KGE = 0.54), with $R^2 = 0.36$ and Pearson $r = 0.60$, indicating limited performance at the finest temporal resolution. This result is consistent with two sources of mismatch: (i) the highly intermittent and event-driven hydrology typical of drier Mediterranean basins, which amplifies the effect of small timing errors at the daily scale, and (ii) the nature of the available observations, which correspond to daily reservoir volume variations rather than unregulated river discharge. Reservoir regulation integrates inflows and operational releases, introducing day-to-day changes not explicitly simulated by the catchment model and therefore penalizing daily efficiency metrics. Model performance improved markedly at the monthly scale (NSE = 0.46; $R^2 = 0.67$; Pearson $r = 0.82$), indicating that the model satisfactorily represents the dominant seasonal-to-interannual water balance dynamics of the Siurana catchment (see Fig. 5).

290 [Figure 5 about here.]

295 Overall, the hydrological calibration based solely on river discharge provided a consistent and physically meaningful representation of catchment water balance in both systems, particularly at the monthly scale. Nevertheless, it should be noted that different parameter combinations may yield comparable performance metrics (i.e., equifinality), and thus the calibrated parameter set should be interpreted as one plausible representation of the system rather than a unique solution.

300 Furthermore, the differences in calibrated parameter values between catchments highlight the limited transferability of parameter sets across contrasting hydro-climatic conditions. While some parameters (e.g., conductivity multipliers) remained consistent, others required substantial adjustment, suggesting that catchment-specific calibration remains necessary to adequately capture local hydrological behavior.

4.2.2 Independent evaluation of plant dynamics using LAI and GPP

305 Following hydrological calibration and validation, the plant dynamics component of the model was evaluated independently by comparing simulated LAI and GPP against remotely sensed observations. Neither LAI nor GPP data were used during model calibration, allowing for an unbiased assessment of vegetation dynamics emerging from the simulated water and energy fluxes.



[Figure 6 about here.]

[Figure 7 about here.]

310 Model performance was evaluated at the grid-point level using monthly time series, with R^2 and RMSE used to quantify agreement between simulated and observed values (see Figs. 7 and 6).

Across both catchments, simulated GPP showed consistently stronger agreement with observations than simulated LAI. This is expected from the underlying processes: GPP dynamics are strongly governed by the seasonal climatic signal, and the model can capture the effect of climate drivers on photosynthesis relatively well. LAI dynamics are intrinsically more difficult to reproduce, particularly the intra-annual variation in evergreen species and the interannual response to drought stress—
315 which requires accurate simulation of drought-induced defoliation and recovery during subsequent wet periods. Improving the representation of these defoliation and recovery processes in the model remains an objective for future development.

Simulated LAI exhibited greater spatial variability in performance, with moderate correlations and localized areas of higher RMSE in both catchments. While the model captured the main seasonal patterns of canopy development, these results suggest that structural vegetation properties are more challenging to simulate accurately than flux-based variables such as GPP,
320 particularly at fine spatial scales.

4.3 Overall effects of forest management

Forest management produced coherent ecohydrological responses in both catchments, reducing canopy structure and altering water partitioning and fire-related conditions (Table 5). Management was applied only in stands where structural thresholds were reached, affecting approximately 4 950 ha of the 12 575 ha simulated in Aigua d’Ora and 1 350 ha of the 6 075 ha
325 simulated in Siurana (Table 1). Although interventions covered a substantial fraction of both landscapes, the magnitude of the response differed between basins.

[Table 5 about here.]

In Aigua d’Ora, management caused marked reductions in vegetation structure and productivity. LAI decreased by -10.2% (mean difference $-0.20 \text{ m}^2 \text{ m}^{-2}$), accompanied by a reduction in GPP of -7.4% ($\approx -10.5 \text{ gC m}^{-2} \text{ d}^{-1}$). These structural
330 changes translated into a clear increase in catchment blue-water fluxes: deep drainage increased by $+9.4\%$ ($+2.88 \text{ mm}$) and runoff by $+4.7\%$ ($+0.28 \text{ mm}$). Relative water content (RWC) also increased ($+1.86\%$), indicating improved vegetation water status following biomass removal and reduced competition for soil water.

In Siurana, management effects were smaller but directionally consistent. LAI decreased by -3.1% ($-0.06 \text{ m}^2 \text{ m}^{-2}$) and GPP declined by -1.8% . Hydrological variables also shifted toward increased water availability: deep drainage increased by
335 $+1.5\%$ ($+0.32 \text{ mm}$) and runoff by $+0.5\%$ ($+0.02 \text{ mm}$), while RWC increased marginally ($+0.55\%$).

Fire behavior indicators also responded to management. In both catchments, crown fire Byram intensity ($I_{b,\text{crown}}$) decreased under the managed scenario, reflecting reduced canopy fuel continuity and lower available canopy fuel loads. The reduction was particularly pronounced in Aigua d’Ora (-27.2%) while in Siurana the decrease was smaller (-6.0%) but still evident. Surface



340 fire Byram intensity ($I_{b,surface}$) showed more limited changes (-4.0% and $+1.7\%$, respectively), suggesting that management primarily reduced the potential severity of crown fires while having a weaker and more site-dependent influence on surface fire intensity.

[Table 6 about here.]

Fuel moisture responses differed between catchments. In Aigua d'Ora, canopy fuel moisture content (CFMC) decreased slightly under management (-0.2% overstory, -0.9% understory), whereas in Siurana both overstory and understory CFMC 345 increased marginally ($+0.2\%$ and $+0.4\%$, respectively). It is worth noting that changes in CFMC may partly reflect shifts in species composition resulting from differential thinning intensities, since different species have different maximum live fuel moisture values ($LFMC_{max}$), rather than (or in addition to) a direct effect of improved plant water status.

When considering the entire simulation period, management effects are dominated by structural and hydrological responses. However, differences become more pronounced during summer months, when fire risk is highest (Table 6). During this pe- 350 riod, the reduction in crown fire intensity is particularly relevant, as lower canopy fuel loads and reduced canopy continuity limit the potential for crown fire development. While annual-average changes in fire-related variables may appear moderate, management can substantially influence fire behavior under peak fire-weather conditions.

A noteworthy anomaly emerges in the summer hydrological response of the Siurana catchment: whereas annual-average runoff increased slightly under management ($+0.5\%$), summer runoff showed a small but opposite response (-3.1% ; -0.04 355 mm). Crucially, this runoff reduction coincides with increases in both vegetation water status and subsurface fluxes: relative water content (RWC) increased by $+0.70\%$ and deep drainage increased by $+1.65\%$ ($+0.09$ mm) under management during summer. This pattern suggests that the water freed by thinning — through reduced canopy interception — reaches the soil surface and is partitioned preferentially towards infiltration and subsurface pathways (improving soil moisture and deep drainage) rather than towards surface runoff. Part of the additional soil water is taken up by the remaining vegetation, improving its 360 water status (higher RWC), while the rest percolates towards deeper layers (higher deep drainage). The net result is a redistribution of water away from surface runoff and towards subsurface storage and plant uptake, consistent with the dominance of drought-tolerant deep-rooted species in Siurana, particularly *Quercus ilex*. This pattern is discussed further in Sect. 5.3.

5 Discussion

The observed increase in LAI without a corresponding rise in GPP is consistent with well-established eco-physiological mech- 365 anisms and does not represent a contradiction. As canopy density increases, light penetration within the canopy declines due to self-shading, leading to saturation of photosynthetic rates while additional foliage contributes little to further carbon assimilation (Bouriaud et al., 2016). Moreover, increases in leaf biomass raise autotrophic respiration costs, which can offset potential gains in photosynthesis (DeLUCIA et al., 2007). Consequently, structural vegetation greening may occur without proportional increases in ecosystem productivity.

370 Such structural–physiological decoupling between canopy density and carbon assimilation has been widely reported, particularly in water-limited environments. While LAI represents a structural ecosystem attribute, GPP reflects physiological

functioning, which can become constrained by water availability and atmospheric demand (Yuan et al., 2019; Hu et al., 2022). In Mediterranean ecosystems, where summer drought frequently limits photosynthetic activity, increases in vegetation density therefore do not necessarily translate into enhanced ecosystem productivity.

375 The combined trend analysis and model simulations support a coherent mechanistic interpretation linking vegetation structure, hydrology, and fire behavior. The long-term increase in LAI indicates progressive forest densification, which can increase catchment water consumption through higher transpiration demand and enhanced canopy storage. As a result, greater vegetation water use may reduce blue-water availability and contribute to declining river discharge, even in the absence of significant trends in precipitation or temperature. Similar patterns of vegetation greening accompanied by limited productivity gains and
380 declining streamflow have been documented across semi-arid and temperate catchments worldwide (Ukkola et al., 2016; Xiao et al., 2024; Pang et al., 2023; Yu et al., 2024; Jia et al., 2025).

The forest management simulations provide an additional test of this mechanism. By reducing canopy density and transpiring surface area, thinning decreases vegetation water demand and modifies rainfall partitioning, leading to modest but consistent increases in runoff and deep drainage. These results indicate that a hydrologically calibrated model can generate realistic plant
385 dynamics, supporting its use for integrated analyses of water–vegetation interactions and long-term ecohydrological responses under Mediterranean climate conditions.

5.1 Model performance and comparison with the literature

Hydrological performance obtained in this study is consistent with values commonly reported for hydrological and ecohydrological models applied in Mediterranean environments. In Aigua d’Ora, daily model performance (NSE = 0.49; KGE = 0.61)
390 falls within the typical range reported for models such as SWAT and TETIS in semi-arid Mediterranean catchments (Pulighe et al., 2019; Francés et al., 2007; Vélez et al., 2009). Model performance improved when discharge was aggregated to the monthly scale, reflecting the expected reduction in timing errors associated with daily hydrological variability.

Lower daily performance in the Siurana catchment (NSE = 0.15) can be partly attributed to reservoir regulation, as discussed in the Results section. The improved monthly performance (NSE = 0.46) provides a more appropriate indicator of the model’s
395 ability to reproduce the dominant water balance dynamics of the catchment.

Independent evaluation of simulated vegetation dynamics further supports the realism of the model. Simulated GPP showed good agreement with remotely sensed observations, comparable to results reported for both light-use efficiency models and process-based ecohydrological models such as RHESSys (Tague and Band, 2004; Zierl and Bugmann, 2007; Cicuéndez et al., 2024). In contrast, simulated LAI showed greater spatial variability, which is a common outcome when comparing structural
400 vegetation variables derived from forest inventory data with satellite-derived products (Ruiz-Pérez et al., 2017). Importantly, neither LAI nor GPP observations were used during model calibration, indicating that vegetation dynamics emerge from the ecohydrological constraints represented in the model rather than from parameter fitting to satellite data.



5.2 Hydrological impacts of forest management

Management impacts can be interpreted through a coupled structural–hydrological–fire pathway. By reducing canopy density
405 (LAI and stand biomass), thinning lowers transpiration demand and modifies rainfall partitioning, which can increase the
fraction of water routed to runoff and deep drainage at the catchment scale. In parallel, thinning alters fuel structure by reducing
canopy fuel continuity and canopy fuel loads, which directly affects potential fire behavior, reflected here by changes in crown
and surface Byram intensity (Byram, 1959). Thinning also reduces canopy fuel moisture content (CFMC), contributing to
increased fire hazard when considered in isolation, although this effect may partly reflect shifts in species composition rather
410 than a direct response of individual plant water status.

Forest management reduced canopy water use primarily through decreases in LAI and transpiring biomass, consistent with
experimental and modelling evidence showing that thinning reduces evapotranspiration by lowering canopy leaf area and tran-
spiration demand (Bosch and Hewlett, 1982; González-Sanchis et al., 2015; del Campo et al., 2018; Brown et al., 2005).
Because thinning was triggered dynamically when structural thresholds were exceeded, management was spatially heteroge-
415 neous and affected 39.4% of Aigua d’Ora and 22.2% of Siurana. The lower treated fraction in Siurana likely reflects the slower
stand growth expected under stronger climatic water limitation, which reduces the frequency with which the species-specific
basal area thresholds are exceeded over the simulation period.

Across the full simulation period, management increased blue-water fluxes in both catchments, although the magnitude
of the response differed substantially. In the wetter Aigua d’Ora basin, canopy reductions produced clear increases in deep
420 drainage and runoff together with improved vegetation water status (higher RWC). In contrast, responses in the drier Siurana
catchment were smaller, reflecting stronger climatic water limitation and the smaller proportion of treated stands.

Species composition may further contribute to this difference. The prevalence of *Quercus ilex* in Siurana likely buffers the
hydrological response because this species can access deeper soil water reserves and maintain transpiration during drought
(Vicente et al., 2018). In mixed stands, such deep-rooted species may sustain water use even after canopy thinning, reducing
425 the sensitivity of catchment water yield to structural changes. These results highlight the strong context dependency of hy-
drological responses to forest management. Similar findings have been reported across Mediterranean and other water-limited
environments, where the magnitude of water yield changes following vegetation reduction depends strongly on climate, soil
water storage capacity, vegetation type, and the proportion of the catchment affected by management (Farley et al., 2005;
Del Campo et al., 2022).

430 At the same time, reductions in canopy fuel loads and canopy continuity decrease crown fire Byram intensity (Byram, 1959),
indicating lower potential crown-fire intensity. These effects are particularly relevant during summer months, when evaporative
demand is highest and wildfire hazard peaks.

5.3 Carbon–water trade-offs

In such environments, reductions in canopy density may primarily alleviate vegetation water stress rather than generate signifi-
435 cant increases in catchment-scale water yield (Vicente et al., 2018). This pattern may be further explained by the dominance of



Quercus ilex in the Siurana catchment, a drought-tolerant anisohydric species characterised by deep root systems (up to 13 m) that allow access to groundwater and maintenance of physiological activity during summer drought periods (Vicente et al., 2018). Unlike isohydric species such as pines, *Q. ilex* maintains gas exchange rates under intense water stress through delayed stomatal closure (Vicente et al., 2018), and forest management has been shown to increase rather than reduce individual water
440 consumption in this species without altering its water-use strategy (Vicente et al., 2018). Moreover, empirical evidence from thinning experiments in low-biomass semiarid *Q. ilex* forests shows that gains in net precipitation are progressively dampened over time by the crown growth of remaining trees (del Campo et al., 2018), suggesting that water released by removed individuals is rapidly taken up by the residual stand, thereby limiting any catchment-scale hydrological response. We additionally
445 hypothesise that the resprouting capacity of *Q. ilex* — a well-documented trait allowing rapid regeneration from lignotubers and root sprouts following disturbance — may further attenuate the long-term hydrological benefit of thinning in Siurana. If resprouting individuals progressively reclaim the space and resources freed by the intervention, canopy closure would accelerate and the structural impact of management on LAI would diminish over time. Since the simulations include forest dynamics, this response is at least partly captured in the model, although dedicated analyses of the temporal evolution of LAI in managed stands would be needed to confirm this mechanism.

450 This mechanism offers a plausible explanation for the summer response pattern observed in Siurana: runoff decreased marginally (-3.1%) while deep drainage increased ($+1.65\%$) and vegetation water status improved (RWC $+0.70\%$). The coherent interpretation is that thinning, by reducing canopy interception, allows more precipitation to reach the soil surface during summer storms. This additional water is then routed preferentially through subsurface pathways: part is taken up by the remaining vegetation — which, due to the anisohydric strategy and deep-rooting habit of *Q. ilex*, readily intensifies transpiration
455 and water uptake from deep layers once inter-tree competition is reduced — thereby improving plant water status (higher RWC); the rest percolates to deeper soil layers, increasing deep drainage. Surface runoff, which in this dry catchment depends primarily on saturation-excess mechanisms during intense rainfall events, is not enhanced by this infiltration-dominated response and in fact decreases slightly. The net effect is therefore a redistribution of the water freed by management away from surface pathways and towards subsurface storage and plant uptake — an outcome that is ecologically meaningful (reduced
460 vegetation water stress) but runs counter to the conventional expectation of increased water yield following canopy removal. This behavior highlights how deep-rooting and anisohydric traits, exemplified by *Q. ilex*, can determine both the direction and the pathway of hydrological responses to forest management under peak drought conditions, and underscores the importance of accounting for vegetation composition in the design of thinning strategies in water-limited Mediterranean catchments.

5.4 Implications for Mediterranean forest management

465 Mediterranean forests are increasingly managed to mitigate drought stress and wildfire risk under climate change. The results presented here indicate that thinning can simultaneously influence hydrological processes and potential fire behavior. By reducing canopy fuel continuity and canopy fuel loads, management lowered crown fire Byram intensity, particularly in the Aigua d'Ora catchment.



These effects become most relevant during summer months, when fuel moisture is lowest and wildfire hazard peaks. Consequently, annual-average indicators may underestimate the practical relevance of management for fire behavior, whereas seasonal analyses provide more decision-relevant information.

However, hydrological benefits of thinning cannot be generalized across landscapes. As demonstrated here, ecohydrological responses depend strongly on climatic conditions, vegetation composition, and the spatial distribution of treated stands. Adaptive forest management strategies should therefore incorporate catchment-scale ecohydrological diagnostics in order to identify where thinning interventions can simultaneously improve water availability, reduce wildfire hazard, and minimize productivity losses.

5.5 Suitability of MEDFATELAND for catchment-scale vegetation–water analysis

This study demonstrates that MEDFATELAND is suitable for analysing coupled vegetation and water dynamics at the catchment scale in Mediterranean environments. After calibration using river discharge only, the model reproduced the dominant hydrological variability—particularly at monthly and seasonal scales—and generated realistic spatial and temporal patterns of vegetation activity (LAI and GPP) without using vegetation observations during calibration. This independent agreement supports the internal consistency of the representation of water, energy, and plant physiological processes, and indicates that simulated vegetation dynamics emerge from ecohydrological constraints rather than parameter fitting to satellite products.

The added value of the distributed formulation goes beyond reproducing outlet discharge. A lumped model could be calibrated to match catchment streamflow, but it would not allow evaluating the spatial realism of vegetation dynamics, nor representing management as a spatially heterogeneous intervention. The distributed configuration enabled (i) pixel-level evaluation of LAI and GPP, (ii) representation of spatially variable forest structure and species composition, and (iii) quantification of how local canopy reductions translate into catchment-scale changes in runoff and deep drainage.

6 Conclusions

This study evaluated the capability of the distributed ecohydrological model MEDFATELAND to simulate coupled vegetation and hydrological dynamics at the catchment scale and explored the potential impacts of forest management on water balance and fire-related variables in two Mediterranean basins.

The model reproduced the main hydrological dynamics of both catchments with moderate performance at the daily scale and improved agreement at the monthly scale. Importantly, the model also generated realistic vegetation dynamics, reproducing spatial and temporal patterns of GPP and LAI without using vegetation observations during calibration. This independent agreement supports the internal consistency of the ecohydrological processes represented in the model.

Trend analyses revealed a significant increase in LAI over the last two decades without corresponding increases in GPP, suggesting a structural densification of forests without proportional gains in productivity. This vegetation greening coincided with declining river discharge despite the absence of significant trends in precipitation or temperature, indicating that increasing vegetation water consumption may be contributing to reduced catchment water yield.



505

Simulated forest management scenarios consistently reduced canopy density while slightly increasing blue-water fluxes, including runoff and deep drainage. These hydrological benefits were more pronounced in the wetter Aigua d’Ora catchment, whereas responses in the drier Siurana basin were smaller but directionally consistent. The results highlight that the hydrological effectiveness of thinning depends strongly on climatic conditions, vegetation composition, and the spatial extent of treated areas.

Management also influenced simulated fire behavior by reducing crown fire Byram intensity (Byram, 1959), reflecting decreased canopy fuel continuity and lower canopy fuel loads in managed stands. These reductions were particularly evident in Aigua d’Ora and become especially relevant during summer months, when fuel moisture is lowest and wildfire risk is highest.

510

Overall, this work demonstrates that MEDFATELAND provides a suitable framework for analyzing vegetation–water interactions and evaluating forest management strategies at the watershed scale. A key advantage of the distributed approach is that it enables spatial evaluation of vegetation dynamics and spatially explicit representation of management interventions—capabilities that cannot be addressed with catchment-aggregated models calibrated only at the outlet.

515

Future work should explore a broader range of management scenarios (varying treatment intensity, spatial extent, and timing) and assess long-term ecohydrological responses under projected climate conditions, in order to better inform adaptive forest management strategies in Mediterranean forests facing increasing drought stress and wildfire risk. By combining model evaluation with scenario analysis, results such as those presented here support the potential of distributed ecohydrological modelling as a decision-support tool for managing Mediterranean forests under increasing drought and fire risk.

Code availability. MEDFATE and MEDFATELAND are open-source R packages distributed via CRAN and GitHub (<https://emf-creaf.github.io/medfateland/>)

520

Data availability. The daily meteorological data used in this study were obtained from the METEOCAT network of weather stations (Servei Meteorològic de Catalunya; <https://www.meteo.cat>) and are available upon request from METEOCAT. Daily streamflow observations for the Aigua d’Ora catchment at the Navès gauging station (EA063) and daily reservoir storage records for the Siurana reservoir were provided by the Agència Catalana de l’Aigua (ACA; <https://aca.gencat.cat>) and are openly accessible. Vegetation dynamics data (LAI and GPP) were obtained from MODIS products MOD15A2H and MOD17A2H (Collection 6.1), distributed by the Land Processes Distributed Active Archive Center (LP DAAC) at <https://lpdaac.usgs.gov>, and are freely available. Soil data were derived from SoilGrids (<https://soilgrids.org>), which is openly accessible. The digital terrain model was derived from airborne LiDAR data from the Plan Nacional de Ortofotografía Aérea (PNOA), available through the Instituto Geográfico Nacional (<https://www.ign.es>). Model input files and simulation scripts are available from the corresponding author upon reasonable request.

530



Author contributions. M. González-Sanchis: Conceptualization, Methodology, Software, Formal analysis, Investigation, Data curation, Writing – original draft, Writing – review & editing, Visualization, Project administration, Funding acquisition. M. De Cáceres: Conceptualization, Methodology, Software, Writing – review & editing, Supervision. P. Martín: Investigation, Data curation, Writing – review & editing, Funding acquisition. G. Piqué: Conceptualization, Writing – review & editing. P. Garcia Iñurria: Writing – review & editing. Susan Manrique: Writing – review & editing.

Competing interests. The authors declare that they have no conflict of interest.

Acknowledgements. This study was carried out within the framework of the research contract *HidroBosc* between the Forest Science and Technology Centre of Catalonia (CTFC) and the Catalan Water Agency (ACA), the research project Boosting process-based models to project forest dynamics and associated ecosystem services at stand-to-regional scales (BOMFORES), funded by the Ministerio de Ciencia e Innovación (PID2021-126679OB-I00; PI: Miquel De Cáceres), and the project ForH2O (2023 CLIMA 0018) funded by the Departament de Recerca i Universitats, d'Acció Climàtica, Alimentació i Agenda Rural i del Fons Climàtic de la Generalitat de Catalunya. The corresponding author was supported by a Torres-Quevedo postdoctoral fellowship (PTQ2022-012708), funded by MCIU/AEI/10.13039/501100011033.

The authors used Claude (Anthropic) to assist with English language editing and improvement of manuscript style and clarity. All scientific content, interpretations, and conclusions are the sole responsibility of the authors.



References

- Agee, J. K. and Skinner, C. N.: Basic principles of forest fuel reduction treatments, *Forest Ecology and Management*, 211, 83–96, 2005.
- Beven, K.: *Rainfall-Runoff Modelling: The Primer*, Wiley-Blackwell, 2nd edn., 2012.
- 550 Bosch, J. M. and Hewlett, J. D.: A review of catchment experiments to determine the effect of vegetation changes on water yield and evapotranspiration, *Journal of Hydrology*, 55, 3–23, [https://doi.org/10.1016/0022-1694\(82\)90117-2](https://doi.org/10.1016/0022-1694(82)90117-2), 1982.
- Bouriaud, O., Teodosiu, M., Kirdeyanov, A. V., and Wirth, C.: A saturating response of photosynthesis to an increasing leaf area index allows selective harvest of trees without affecting forest productivity, *Forest Ecology and Management*, 360, 96–104, <https://doi.org/10.1016/j.foreco.2015.10.037>, 2016.
- 555 Brown, A. E., Zhang, L., McMahon, T. A., Western, A. W., and Vertessy, R. A.: A review of paired catchment studies for determining changes in water yield resulting from alterations in vegetation, *Journal of Hydrology*, 310, 28–61, 2005.
- Byram, G. M.: *Combustion of Forest Fuels*, Tech. rep., USDA Forest Service, New York, 1959.
- Cicuéndez, V., García, M., and Moreno, G.: Modeling Gross Primary Production of a Mediterranean Grassland in Central Spain Using Sentinel-2 NDVI and Meteorological Field Information, *Agronomy*, 14, 321, <https://doi.org/10.3390/agronomy14020321>, 2024.
- 560 Clark, M. P., Nijssen, B., Lundquist, J. D., Kavetski, D., Rupp, D. E., Woods, R. A., Freer, J. E., Gutmann, E. D., Wood, A. W., Brekke, L. D., et al.: A unified approach for process-based hydrologic modeling: I. Modeling concept, *Water Resources Research*, 51, 2498–2514, 2015.
- De Cáceres, M., Martínez-Vilalta, J., Coll, L., Llorens, P., Casals, P., Poyatos, R., Pausas, J. G., and Brotons, L.: Coupling a water balance model with forest inventory data to predict drought stress: the role of forest structural changes vs. climate changes, *Agricultural and forest meteorology*, 213, 77–90, 2015.
- 565 De Cáceres, M., Martín-StPaul, N., Turco, M., Cabon, A., and Granda, V.: Estimating daily meteorological data and downscaling climate models over landscapes, *Environmental Modelling & Software*, 108, 186–196, 2018.
- De Cáceres, M., Mencuccini, M., Martín-StPaul, N., Limousin, J.-M., Coll, L., Poyatos, R., Cabon, A., Granda, V., Forner, A., Valladares, F., et al.: Unravelling the effect of species mixing on water use and drought stress in Mediterranean forests: A modelling approach, *Agricultural and Forest Meteorology*, 296, 108 233, 2021.
- 570 De Cáceres, M., Molowny-Horas, R., Cabon, A., Martínez-Vilalta, J., Mencuccini, M., García-Valdés, R., Nadal-Sala, D., Sabaté, S., Martín-StPaul, N., Morin, X., et al.: Medfate 2.9. 3: a trait-enabled model to simulate mediterranean forest function and dynamics at regional scales. *Geoscientific Model Development*, 16 (11): 3165–3201, 2023. doi: 10.5194, 2023.
- del Campo, A. D., González-Sanchis, M., Lidón, A., Ceacero, C. J., and García-Prats, A.: Rainfall partitioning after thinning in two low-biomass semiarid forests: Impact of meteorological variables and forest structure on the effectiveness of water-oriented treatments, *Journal of Hydrology*, 565, 74–86, 2018.
- 575 Del Campo, A. D., Otsuki, K., Serengil, Y., Blanco, J. A., Yousefpour, R., and Wei, X.: A global synthesis on the effects of thinning on hydrological processes: Implications for forest management, *Forest Ecology and Management*, 519, 120 324, 2022.
- DeLUCIA, E. H., Drake, J. E., Thomas, R. B., and Gonzalez-Meler, M.: Forest carbon use efficiency: is respiration a constant fraction of gross primary production?, *Global Change Biology*, 13, 1157–1167, 2007.
- 580 Farley, K. A., Jobbágy, E. G., and Jackson, R. B.: Effects of afforestation on water yield: A global synthesis with implications for policy, *Global Change Biology*, 11, 1565–1576, <https://doi.org/10.1111/j.1365-2486.2005.01011.x>, 2005.
- Fatichi, S., Pappas, C., and Ivanov, V. Y.: *Modeling plant–water interactions: an ecohydrological overview from the cell to the global scale*, Wiley Interdisciplinary Reviews: Water, 3, 327–368, 2016a.



- Fatichi, S., Vivoni, E. R., Ogden, F. L., Ivanov, V. Y., Mirus, B., Gochis, D., Downer, C. W., Camporese, M., Davison, J. H., Ebel, B., et al.:
585 An overview of current applications, challenges, and future trends in distributed process-based models in hydrology, *Journal of Hydrology*,
537, 45–60, 2016b.
- Francés, F., Vélez, J. I., and Vélez, J. J.: Split-parameter structure for the automatic calibration of distributed hydrological models, *Journal*
of Hydrology, 332, 226 – 240, <https://doi.org/https://doi.org/10.1016/j.jhydrol.2006.06.032>, 2007.
- García-Ruiz, J. M., López-Moreno, J. I., Vicente-Serrano, S. M., Lasanta, T., and Beguería, S.: Mediterranean water resources in a global
590 change scenario, *Earth-Science Reviews*, 105, 121–139, <https://doi.org/10.1016/j.earscirev.2011.01.006>, 2011.
- González-Sanchis, M., Del Campo, A. D., and Molina, A. J.: Modeling adaptive forest management of a semi-arid Mediterranean Aleppo
pine plantation, *Ecological Modelling*, 308, 34–44, <https://doi.org/10.1016/j.ecolmodel.2015.04.002>, 2015.
- Hu, Z., Piao, S., Knapp, A. K., Wang, X., Peng, S., Yuan, W., Running, S., Mao, J., Shi, X., Ciais, P., Huntzinger, D. N., Yang, J., and
Yu, G.: Decoupling of greenness and gross primary productivity as aridity decreases, *Remote Sensing of Environment*, 279, 113 120,
595 <https://doi.org/10.1016/j.rse.2022.113120>, 2022.
- Jia, H., Tian, B., Song, X., Sun, W., and Mu, X.: Hydrological shifts from vegetation restoration in semi-arid regions: Insights from typical
watersheds of the Yellow River, *Ecological Indicators*, 178, 111 746, <https://doi.org/10.1016/j.ecolind.2024.111746>, 2025.
- Kendall, M. G.: *Rank Correlation Methods*, Charles Griffin, London, 4th edn., 1975.
- Lasanta, T., Arnáez, J., Pascual, N., Ruiz-Flaño, P., Errea, M. P., and Lana-Renault, N.: Space-time process and drivers of land abandonment
600 in Europe, *Catena*, 149, 810–823, <https://doi.org/10.1016/j.catena.2016.02.024>, 2017.
- Mann, H. B.: Nonparametric tests against trend, *Econometrica*, 13, 245–259, <https://doi.org/10.2307/1907187>, 1945.
- McLeod, A. I.: Kendall: Kendall rank correlation and Mann-Kendall trend test, <https://CRAN.R-project.org/package=Kendall>, r package
version 2.2, 2011.
- Ostendorf, B. and Reynolds, J. F.: Relationships between a terrain-based hydrologic model and patch-scale vegetation patterns in an arctic
605 tundra landscape, *Landscape Ecology*, 8, 229–237, 1993.
- Pang, X., Liu, Y., Zhang, Q., and Sun, W.: Environmental changes promoted vegetation growth and altered eco-hydrological processes in a
semi-arid region, *Journal of Hydrology*, 621, 129 635, <https://doi.org/10.1016/j.jhydrol.2023.129635>, 2023.
- Pappas, C., Fatichi, S., Rimkus, S., Burlando, P., and Huber, M. O.: The role of local-scale heterogeneities in terrestrial ecosystem modeling,
Journal of Geophysical Research: Biogeosciences, 120, 341–360, 2015.
- 610 Pohlert, T.: trend: Non-parametric trend tests and change-point detection, <https://CRAN.R-project.org/package=trend>, r package version
1.1.6, 2023.
- Pulighe, G., Fiori, M., and Lupia, F.: Predicting Streamflow and Nutrient Loadings in a Semi-Arid Mediterranean Watershed with Ephemeral
Streams Using the SWAT Model, *Agronomy*, 9, 723, <https://doi.org/10.3390/agronomy9110723>, 2019.
- R Core Team: R: A Language and Environment for Statistical Computing, R Foundation for Statistical Computing, Vienna, Austria, <https://www.R-project.org/>, 2024.
- 615 Ruiz-Pérez, G., García-Caparrós, P., and Francés, F.: Coupling distributed hydrological and vegetation models to assess ecohydrological
processes in Mediterranean catchments, *Journal of Hydrology*, 550, 98–113, <https://doi.org/10.1016/j.jhydrol.2017.04.036>, 2017.
- Sen, P. K.: Estimates of the regression coefficient based on Kendall's tau, *Journal of the American Statistical Association*, 63, 1379–1389,
<https://doi.org/10.1080/01621459.1968.10480934>, 1968.
- 620 Sun, G., Wei, X., Hao, L., Sanchis, M. G., Hou, Y., Yousefpour, R., Tang, R., and Zhang, Z.: Forest hydrology modeling tools for watershed
management: A review, *Forest Ecology and Management*, 530, 120 755, 2023.



- Tague, C. L. and Band, L. E.: RHESSys: Regional Hydro-Ecologic Simulation System—An object-oriented approach to spatially distributed modeling of carbon, water, and nutrient cycling, *Earth Interactions*, 8, 1–42, [https://doi.org/10.1175/1087-3562\(2004\)8<1:RRHSA>2.0.CO;2](https://doi.org/10.1175/1087-3562(2004)8<1:RRHSA>2.0.CO;2), 2004.
- 625 Ukkola, A. M., Prentice, I. C., Keenan, T. F., van Dijk, A. I. J. M., Viney, N. R., Myneni, R. B., and Bi, J.: Reduced streamflow in water-stressed climates consistent with CO₂ effects on vegetation, *Nature Climate Change*, 6, 75–78, <https://doi.org/10.1038/nclimate2831>, 2016.
- Vélez, J. I., Puricelli, M., López Unzu, F., and Francés, F.: Parameter extrapolation to ungauged basins with a hydrological distributed model in a Mediterranean region, *Journal of Hydrology*, 372, 353–365, <https://doi.org/10.1016/j.jhydrol.2009.03.052>, 2009.
- 630 Vicente, E., Vilagrosa, A., Ruiz-Yanetti, S., Manrique-Alba, À., González-Sanchís, M., Moutahir, H., Chirino, E., Del Campo, A., and Bellot, J.: Water balance of Mediterranean *Quercus ilex* L. and *Pinus halepensis* Mill. forests in semiarid climates: a review in a climate change context, *Forests*, 9, 426, 2018.
- Wigmosta, M. S., Nijssen, B., Storck, P., and Lettenmaier, D.: The distributed hydrology soil vegetation model, *Mathematical models of small watershed hydrology and applications*, 1, 7–42, 2002.
- 635 Xiao, J., Zhang, Y., Liu, W., and Chen, X.: Responses of hydrological processes to vegetation greening and climate change in subtropical watersheds, *Journal of Hydrology: Regional Studies*, 55, 101 946, <https://doi.org/10.1016/j.ejrh.2024.101946>, 2024.
- Yu, Y., Wang, S., Liu, Y., and Zhang, H.: Divergent changes in vegetation greenness, productivity, and rainfall use efficiency are characteristic of ecological restoration, *Engineering*, 25, 37–49, <https://doi.org/10.1016/j.eng.2023.11.012>, 2024.
- Yuan, W., Zheng, Y., Piao, S., Ciais, P., Lombardozzi, D., Wang, Y., Ryu, Y., Chen, G., Dong, W., Hu, Z., et al.: Increased atmospheric vapor pressure deficit reduces global vegetation growth, *Science advances*, 5, eaax1396, 2019.
- 640 Zierl, B. and Bugmann, H.: Sensitivity of carbon cycling in the European Alps to changes of climate and land cover, *Climatic Change*, 85, 195–212, 2007.

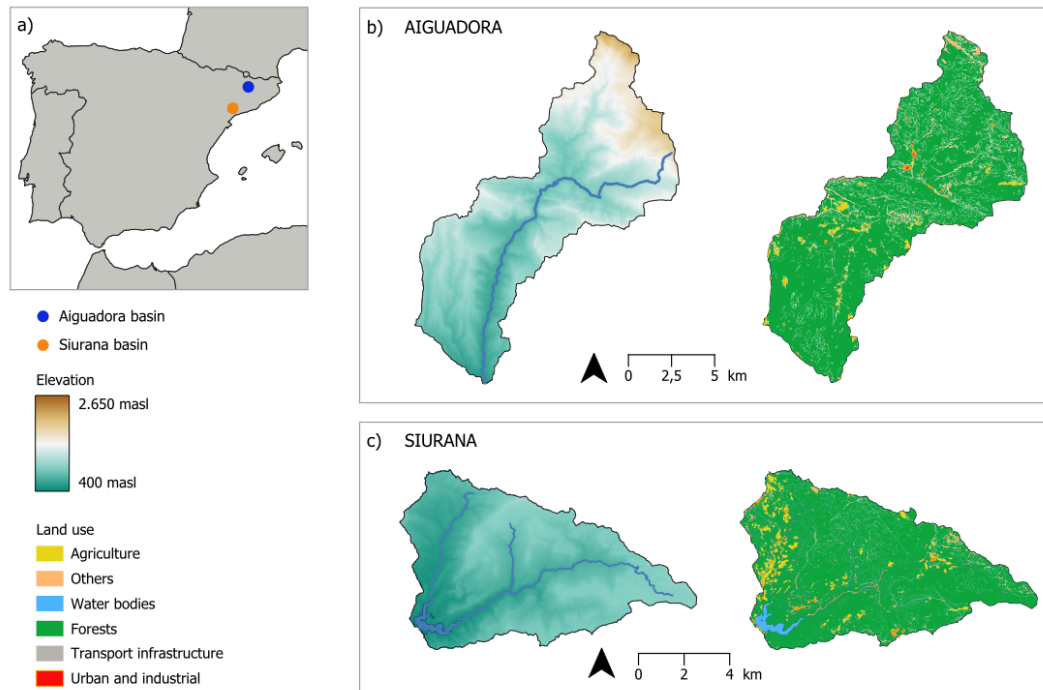


Figure 1. Overview of the study area and its geographical setting

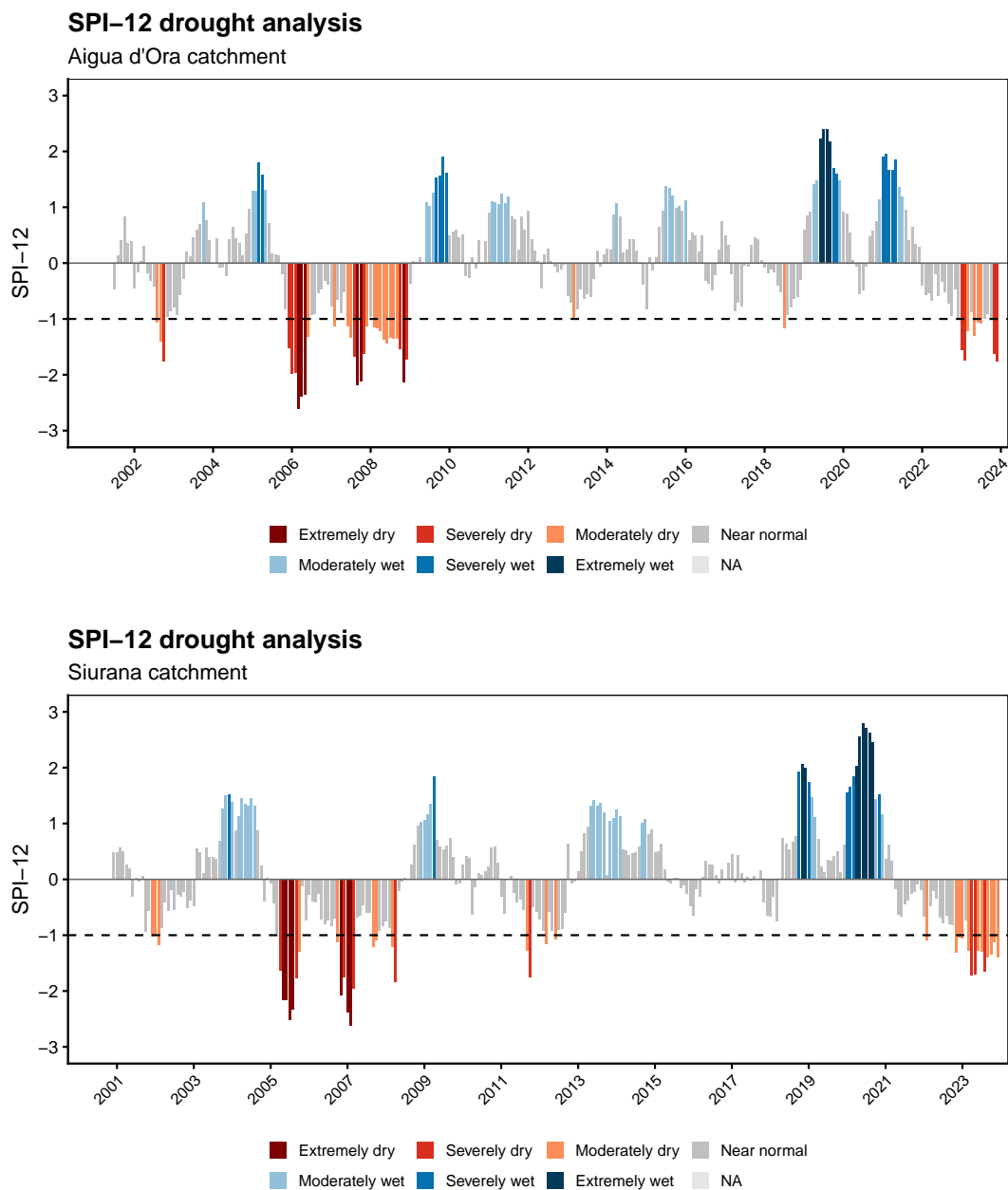
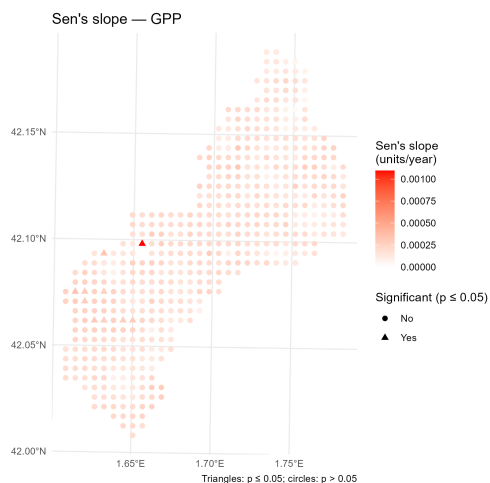
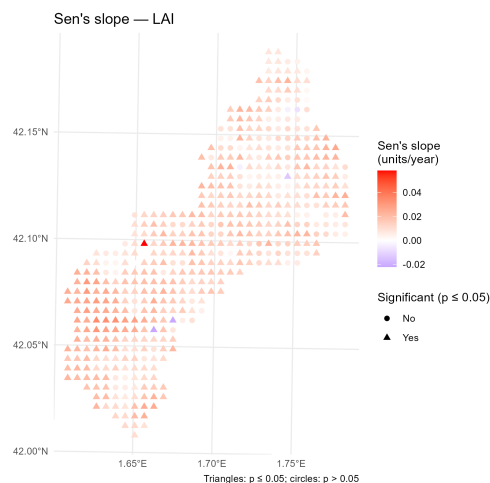


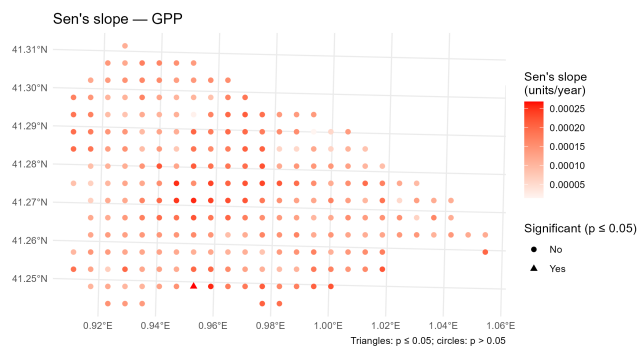
Figure 2. Standardized Precipitation Index at the 12-month scale (SPI-12) for the two study catchments. Negative values indicate dry conditions, with drought defined as $SPI < -1$. Colors represent SPI drought and wetness classes.



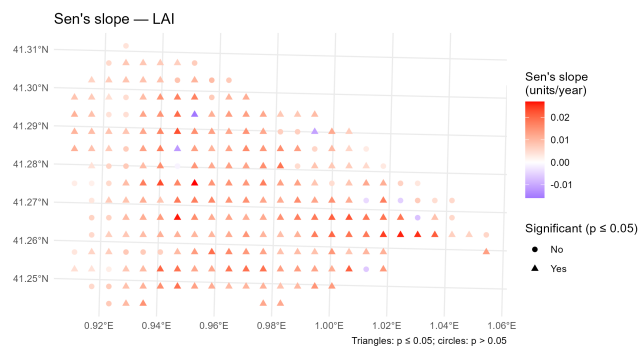
(a) GPP Sen's slope trends at Aigua d'Ora.



(b) LAI Sen's slope trends at Aigua d'Ora.



(c) GPP Sen's slope trends at Siurana.



(d) LAI Sen's slope trends at Siurana.

Figure 3. Spatial distribution of Sen's slope of GPP and LAI trends at Aiguadora ((a) and (b), respectively) and Siurana ((c) and (d), respectively). Values represent annual rates of change. Circles indicate non-significant trends and triangles significant trends ($p < 0.05$). Colour indicates trend direction and magnitude (red: positive; blue: negative).

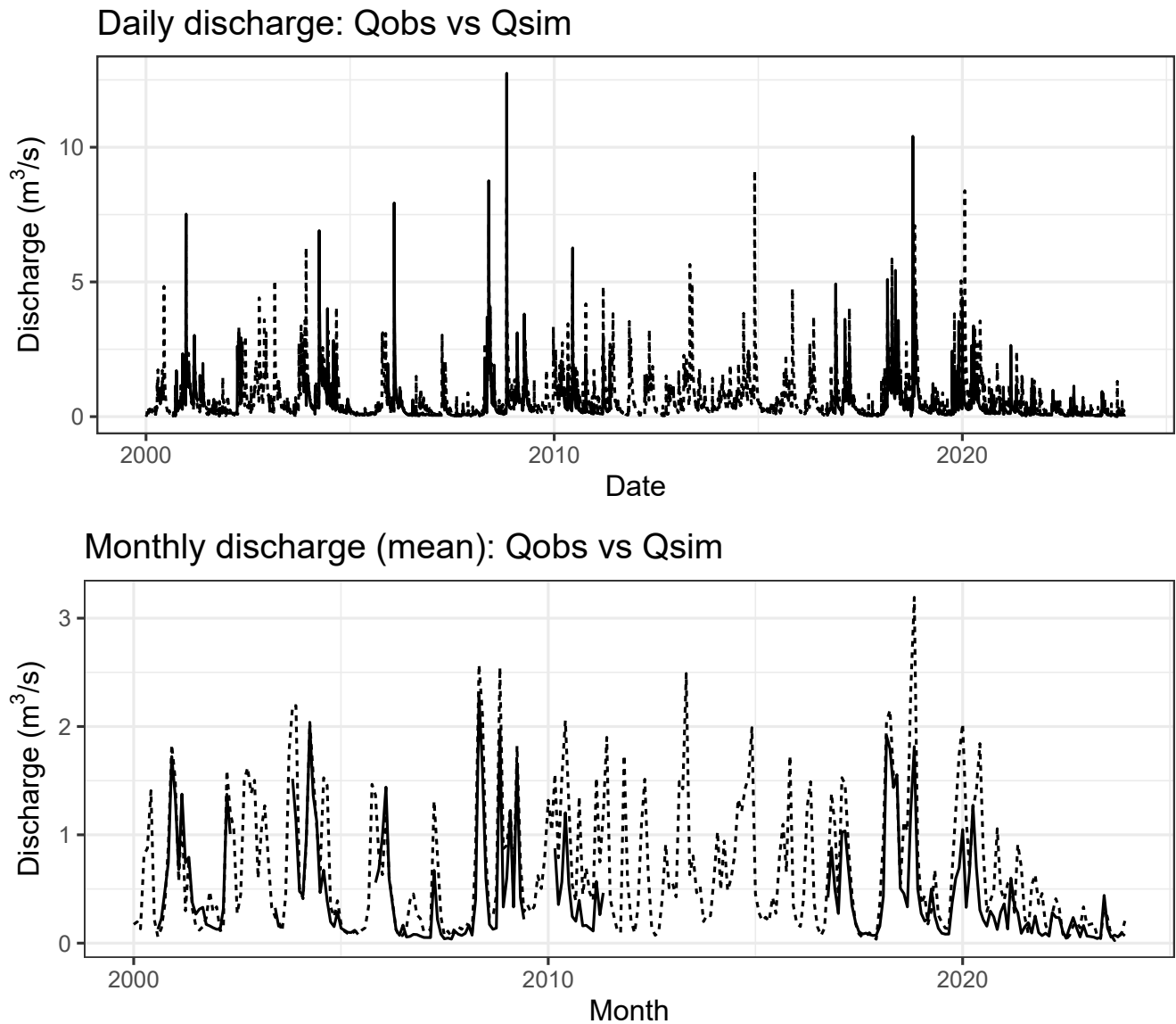


Figure 4. Observed (Q_{obs}) and simulated (Q_{sim}) discharge at Aigua d’Ora catchment under daily and monthly time scales.

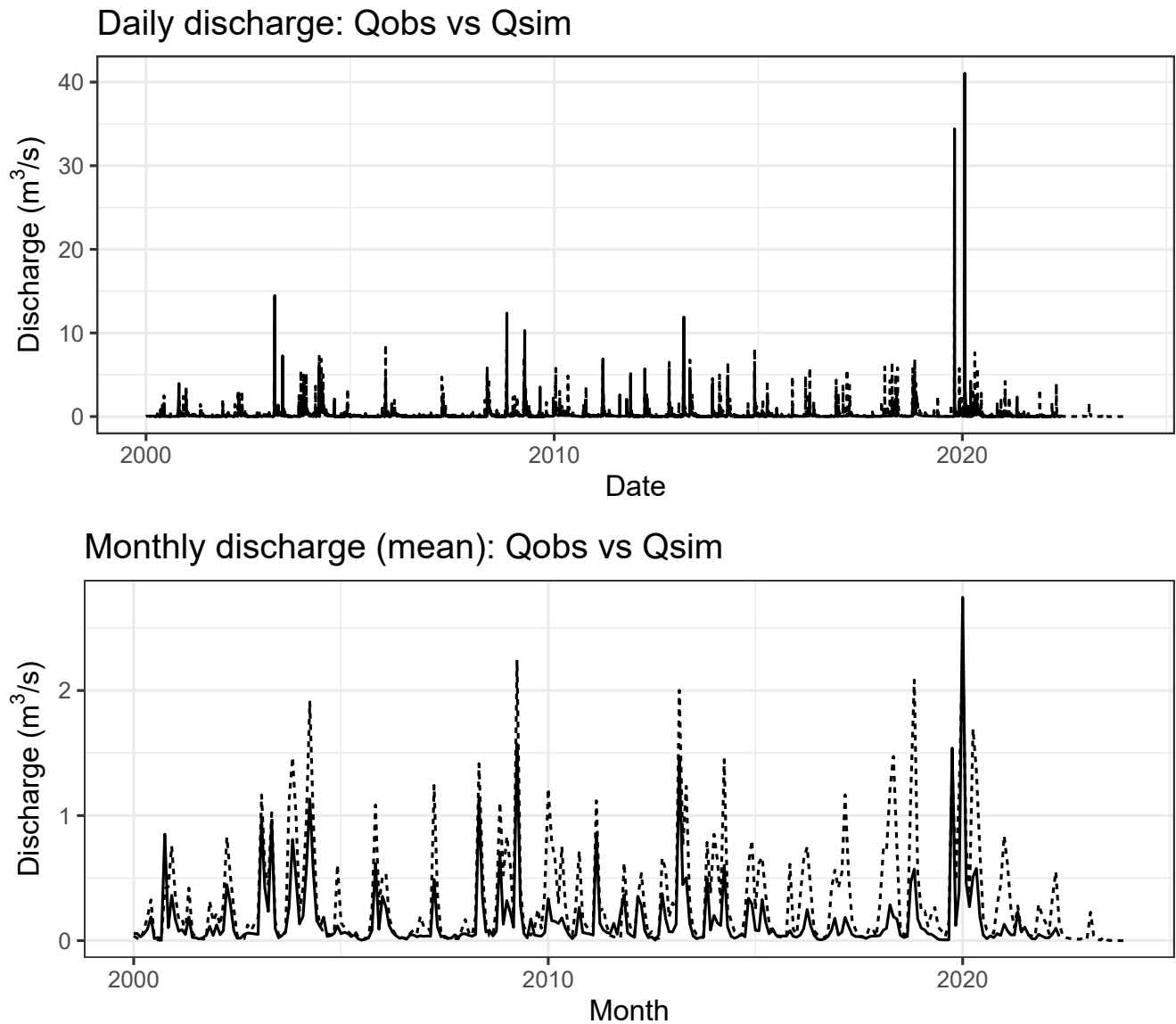


Figure 5. Observed (Q_{obs}) and simulated (Q_{sim}) discharge at Siurana catchment under daily and monthly time scales.

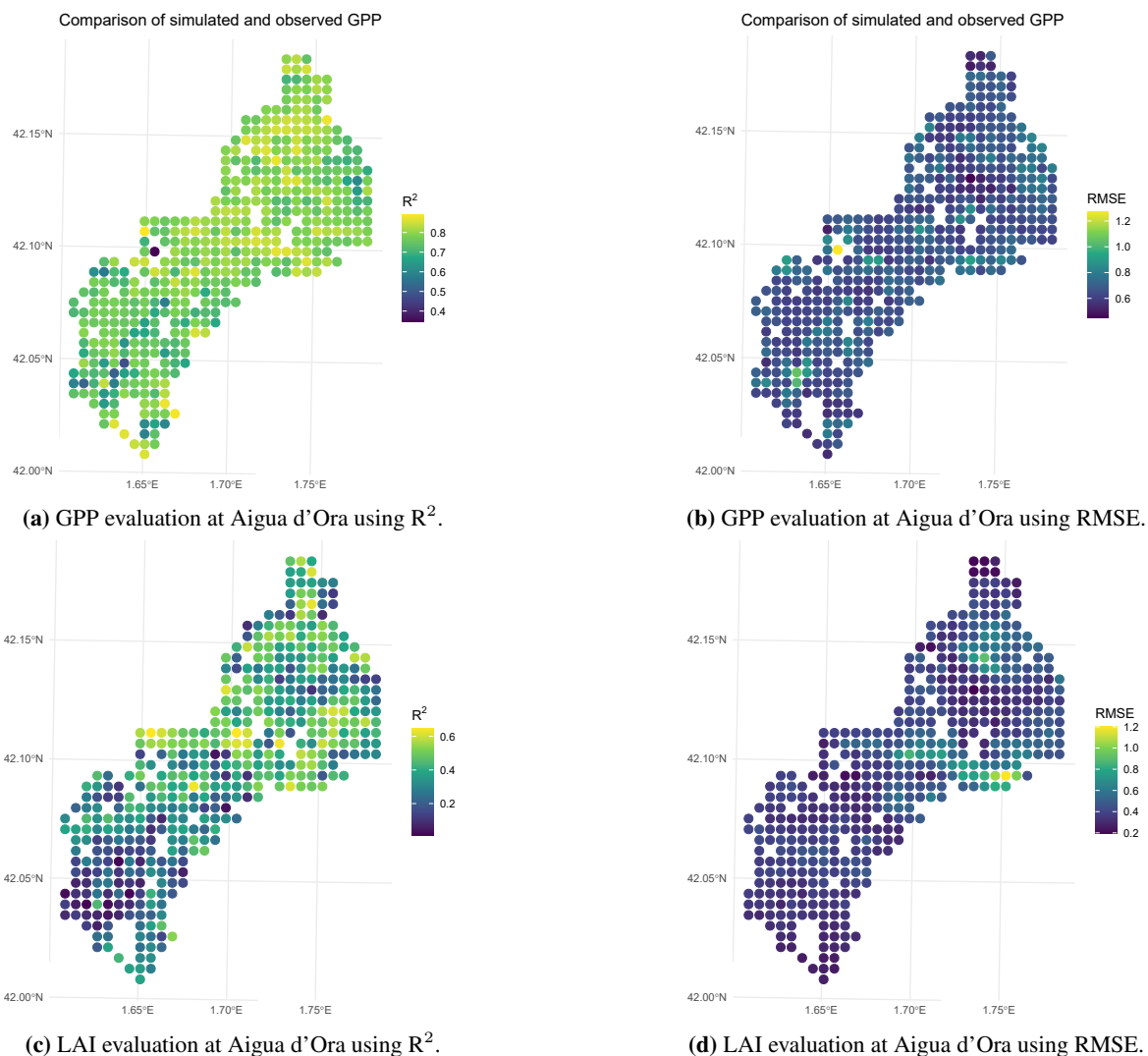
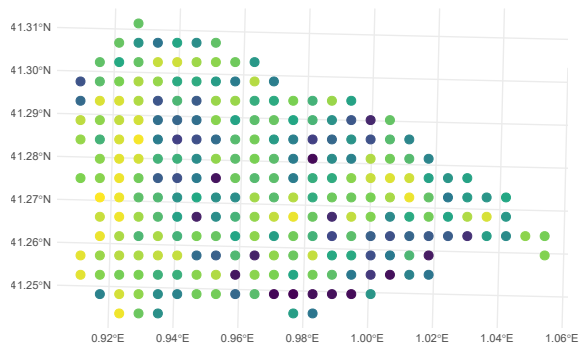
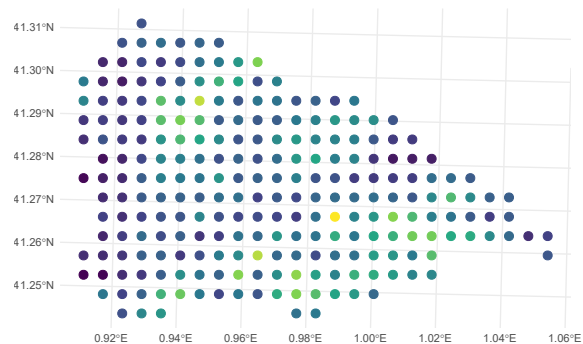


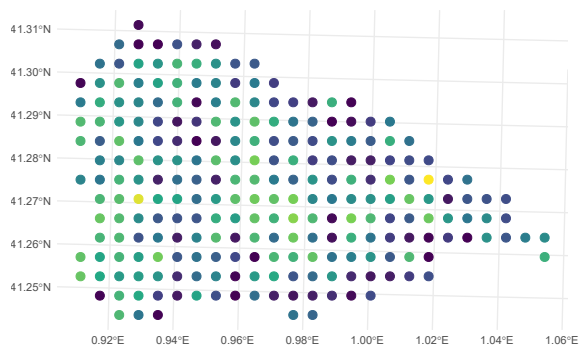
Figure 6. Spatially distributed monthly evaluation of simulated vegetation dynamics at Aiguadora using remotely sensed LAI and GPP. Metrics are computed using monthly time series at the grid-cell level. RMSE units: LAI ($\text{m}^2 \text{m}^{-2}$), GPP ($\text{gC m}^{-2} \text{day}^{-1}$)



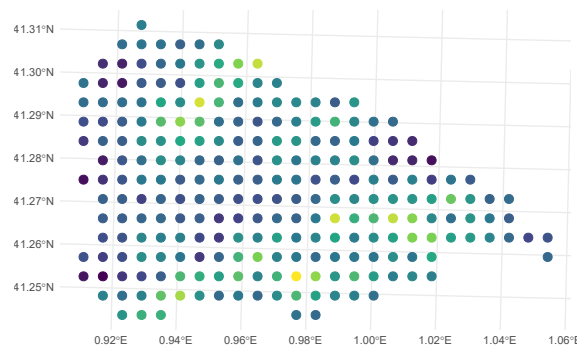
(a) GPP evaluation at Siurana using R^2 .



(b) GPP evaluation at Siurana using RMSE.



(c) LAI evaluation at Siurana using R^2 .



(d) LAI evaluation at Siurana using RMSE.

Figure 7. Spatially distributed monthly evaluation of simulated vegetation dynamics at Siurana using remotely sensed LAI and GPP. Metrics are computed using monthly time series at the grid-cell level. RMSE units: LAI ($\text{m}^2 \text{m}^{-2}$), GPP ($\text{gC m}^{-2} \text{day}^{-1}$)



Table 1. Main physiographic and climatic characteristics of the study catchments.

| Variable | Aigua d'Ora | Siurana |
|-------------------------------------|---|--------------------------------------|
| Catchment area (ha) | 12 575 | 6 075 |
| Managed area (ha) | 4 950 | 1 350 |
| Managed area (%) | 39.4 | 22.2 |
| Mean annual precipitation (mm) | 766 | 530 |
| Mean daily minimum temperature (°C) | 4.9 ± 5.6 | 7.2 ± 5.7 |
| Mean daily maximum temperature (°C) | 14.5 ± 7.2 | 18.3 ± 7.3 |
| Dominant vegetation | <i>Pinus sylvestris</i> , <i>P. nigra</i> | Mediterranean mixed forest/shrubland |
| Hydrological outlet | Navés station | Siurana reservoir |



Table 2. Forest management prescriptions applied in the simulations for the dominant tree species. Thinning operations are triggered when basal area (BA) exceeds the specified threshold.

| Species | Thinning type | BA threshold (m ² ha ⁻¹) | BA removed (%) | Min. interval (years) |
|-------------------------|------------------|--|-------------------|--------------------------|
| <i>Pinus halepensis</i> | below | 19 | 40 | 5 |
| <i>Pinus nigra</i> | above-systematic | 20 | 38 | 5 |
| <i>Pinus sylvestris</i> | below-systematic | 27 | 36 | 5 |
| <i>Pinus uncinata</i> | above-systematic | 28 | 34 | 5 |
| <i>Quercus ilex</i> | systematic | 20 | 45 | 5 |



Table 3. Calibrated hydrological parameters for Aigua d’Ora and Siurana catchments.

| Parameter | Description | Aigua d’Ora | Siurana |
|------------------|---------------------------------|--------------------|----------------|
| $n_{interflow}$ | Interflow exponent | 0.4 | 0.028 |
| $n_{baseflow}$ | Baseflow exponent | 0.5 | 0.5 |
| $R_{localflow}$ | Vertical conductivity factor | 1 | 1 |
| $R_{interflow}$ | Lateral conductivity factor | 8 | 8 |
| $R_{baseflow}$ | Groundwater conductivity factor | 2 | 2 |
| D_{loss} | Deep aquifer loss | 2 | 0.8 |
| $n_{Manning}$ | Manning coefficient | 0.03 | 0.03 |



Table 4. Hydrological model performance for daily and monthly river discharge during the evaluation period. Nash–Sutcliffe Efficiency (NSE), Kling–Gupta Efficiency (KGE), coefficient of determination (R^2), Pearson correlation coefficient (r), and root mean square error (RMSE).

| Catchment | Scale | NSE | KGE | R^2 | Pearson r | RMSE |
|-------------|---------|------|------|-------|-------------|------|
| Aigua d’Ora | Daily | 0.49 | 0.61 | 0.57 | 0.75 | 0.59 |
| Aigua d’Ora | Monthly | 0.62 | 0.56 | 0.75 | 0.87 | 0.39 |
| Siurana | Daily | 0.15 | 0.54 | 0.36 | 0.60 | 0.74 |
| Siurana | Monthly | 0.46 | 0.54 | 0.67 | 0.82 | 0.32 |



Table 5. Comparison of ecohydrological variables between managed (MAN) and non-managed (NoMAN) forest conditions across the two catchments. Values correspond to the whole simulation period. Change (%) is computed as $100 \times (\text{MAN} - \text{NoMAN}) / \text{NoMAN}$.

| Variable | Mean MAN | Mean NoMAN | Difference | Change (%) |
|---|----------|------------|------------|------------|
| Aigua d’Ora | | | | |
| CFMC overstory (%) | 137.29 | 137.55 | -0.25 | -0.18 |
| CFMC understory (%) | 133.53 | 134.73 | -1.21 | -0.90 |
| CFP | 1.55 | 1.54 | +0.01 | +0.65 |
| Deep drainage (mm) | 33.39 | 30.51 | +2.88 | +9.44 |
| GPP ($\text{gC m}^{-2} \text{d}^{-1}$) | 131.22 | 141.74 | -10.52 | -7.42 |
| $I_{b,\text{crown}}$ (kW m^{-1}) | 308.11 | 423.42 | -115.31 | -27.24 |
| $I_{b,\text{surface}}$ (kW m^{-1}) | 56.57 | 58.91 | -2.34 | -3.97 |
| LAI ($\text{m}^2 \text{m}^{-2}$) | 1.77 | 1.96 | -0.20 | -10.20 |
| RWC (%) | 79.52 | 78.07 | +1.45 | +1.86 |
| Runoff (mm) | 6.24 | 5.97 | +0.28 | +4.69 |
| SFP | 1.96 | 2.01 | -0.04 | -1.99 |
| Siurana | | | | |
| CFMC overstory (%) | 124.95 | 124.68 | +0.27 | +0.22 |
| CFMC understory (%) | 117.63 | 117.15 | +0.47 | +0.40 |
| CFP | 2.60 | 2.60 | +0.00 | +0.00 |
| Deep drainage (mm) | 22.20 | 21.88 | +0.32 | +1.46 |
| GPP ($\text{gC m}^{-2} \text{d}^{-1}$) | 117.51 | 119.66 | -2.15 | -1.80 |
| $I_{b,\text{crown}}$ (kW m^{-1}) | 599.18 | 637.40 | -38.22 | -5.99 |
| $I_{b,\text{surface}}$ (kW m^{-1}) | 118.58 | 116.62 | +1.96 | +1.68 |
| LAI ($\text{m}^2 \text{m}^{-2}$) | 1.91 | 1.96 | -0.06 | -3.06 |
| RWC (%) | 62.58 | 62.24 | +0.34 | +0.55 |
| Runoff (mm) | 6.41 | 6.38 | +0.02 | +0.47 |
| SFP | 3.02 | 3.02 | -0.00 | +0.00 |

CFMC: canopy fuel moisture content.

CFP: crown fire potential.

SFP: surface fire potential (maximum of spread potential and flame length).

LAI: leaf area index.

GPP: gross primary production.

RWC: relative water content.

$I_{b,\text{crown}}$ and $I_{b,\text{surface}}$: crown and surface Byram fireline intensity.



Table 6. Comparison of ecohydrological variables between managed (MAN) and non-managed (NoMAN) forest conditions across the two catchments during the summer period (June, July and August). Change (%) is computed as $100 \times (\text{MAN} - \text{NoMAN}) / \text{NoMAN}$.

| Variable | Mean MAN | Mean NoMAN | Difference | Change (%) |
|---|----------|------------|------------|------------|
| Aigua d’Ora | | | | |
| CFMC overstory (%) | 137.57 | 137.85 | -0.28 | -0.20 |
| CFMC understory (%) | 134.03 | 135.33 | -1.30 | -0.96 |
| CFP | 2.16 | 2.12 | +0.03 | +1.62 |
| Deep drainage (mm) | 25.90 | 24.15 | +1.75 | +7.25 |
| GPP ($\text{gC m}^{-2} \text{d}^{-1}$) | 205.90 | 213.10 | -7.20 | -3.38 |
| $I_{b,\text{crown}}$ (kW m^{-1}) | 543.61 | 646.98 | -103.37 | -15.98 |
| $I_{b,\text{surface}}$ (kW m^{-1}) | 99.75 | 101.56 | -1.81 | -1.78 |
| LAI ($\text{m}^2 \text{m}^{-2}$) | 2.19 | 2.31 | -0.12 | -5.14 |
| RWC (%) | 76.30 | 75.17 | +1.13 | +1.51 |
| Runoff (mm) | 5.27 | 5.10 | +0.16 | +3.23 |
| SFP | 3.05 | 3.07 | -0.01 | -0.42 |
| Siurana | | | | |
| CFMC overstory (%) | 125.13 | 124.85 | +0.28 | +0.22 |
| CFMC understory (%) | 117.44 | 116.67 | +0.77 | +0.66 |
| CFP | 3.31 | 3.29 | +0.02 | +0.57 |
| Deep drainage (mm) | 5.61 | 5.52 | +0.09 | +1.65 |
| GPP ($\text{gC m}^{-2} \text{d}^{-1}$) | 169.13 | 171.00 | -1.87 | -1.09 |
| $I_{b,\text{crown}}$ (kW m^{-1}) | 998.40 | 1041.11 | -42.71 | -4.10 |
| $I_{b,\text{surface}}$ (kW m^{-1}) | 230.83 | 227.04 | +3.79 | +1.67 |
| LAI ($\text{m}^2 \text{m}^{-2}$) | 2.31 | 2.35 | -0.05 | -1.97 |
| RWC (%) | 57.96 | 57.56 | +0.40 | +0.70 |
| Runoff (mm) | 1.27 | 1.31 | -0.04 | -3.05 |
| SFP | 4.35 | 4.36 | -0.02 | -0.35 |

CFMC: canopy fuel moisture content.

CFP: crown fire potential.

SFP: surface fire potential (maximum of spread potential and flame length).

LAI: leaf area index.

GPP: gross primary production.

RWC: relative water content.

$I_{b,\text{crown}}$ and $I_{b,\text{surface}}$: crown and surface Byram fireline intensity.